

Adaptive Height Optimisation for Cellular-Connected UAVs using Reinforcement Learning

Erika Fonseca*, Boris Galkin*, Luiz A. DaSilva[†], Ivana Dusparic*

* CONNECT - Trinity College Dublin, Ireland,

[†]Commonwealth Cyber Initiative, Virginia Tech, USA

{fonsecae, galkinb, duspari}@tcd.ie, ldasilva@vt.edu

This work has been submitted to the IEEE for possible publication. Copyright may be transferred without notice, after which this version may no longer be accessible.

Abstract—With the increasing number of Unmanned Aerial Vehicles (UAVs) as users of the cellular network, the research community faces particular challenges in providing reliable UAV connectivity. A challenge that has limited research is understanding how the local building and Base Station (BS) density affects UAV's connection to a cellular network, that in the physical layer is related to its spectrum efficiency. With more BSs, the UAV connectivity could be negatively affected as it has Line-of-Sight (LoS) to most of them, decreasing its spectral efficiency. On the other hand, buildings could be blocking interference from undesirable BS, improving the link of the UAV to the serving BS. This paper proposes a Reinforcement Learning (RL)-based algorithm to optimise the height of a UAV, as it moves dynamically within a range of heights, with the focus of increasing the UAV spectral efficiency. We evaluate the solution for different BS and building densities. Our results show that in most scenarios RL outperforms the baselines achieving up to 125% over naive constant baseline, and up to 20% over greedy approach with up front knowledge of the best height of UAV in the next time step.

Index Terms—Drone, UAV, BS density, Building density, Reinforcement Learning, UAV as end-user.

I. INTRODUCTION

Unmanned Aerial Vehicles (UAVs) can leverage 5G connectivity to perform security surveillance, search and rescue operations, building inspections (roofs, chimneys, siding), agricultural surveys, mapping, delivery of goods, live streaming of shows and events, etc. However, it is still unclear how to provide reliable connectivity to UAVs, as they present a paradigm shift when compared to the usual smartphones. Release 14 of 3GPP [1] states that a UAV needs to maintain continuous connectivity with the mobile network while flying with speeds up to 300km/h.

Previous work, e.g., [2], [3], investigates the feasibility of the use of current network infrastructure to deliver wireless connectivity for UAVs. These studies conclude that currently deployed networks would need to adapt some of their design configurations, such as increasing Base Station (BS) height [4] or changing the tilt of the antennas [5], in order to enable connectivity to UAVs. Redesigning the terrestrial network infrastructure may be unfeasible, and an adaptable solution on

the UAV side may be necessary to accelerate UAV integration into the network.

Qualcomm has carried out several experiments investigating the feasibility of providing a connection to UAVs through the side lobes of BS antennas that have the main lobe directed towards street level, where Ground User Equipment (GUE) typically operates. Preliminary results show that the coverage is adequate for UAVs flying up to 120 m above ground [6]. However, at higher heights the increased line-of-sight (LoS) to different BSs generates high levels of interference at the UAVs. The work of [4] states that, depending on the BS density and height, there is an optimal height at which the UAV should fly to maintain reliable communication. In [7] authors show that the vertical movements of the UAV affect their coverage probability. A UAV can fly over different environments where the local BS density can change, which will force it to change its height to optimise its wireless link to the network, with respect to the local environmental conditions.

To date, no other work addresses adaptive height optimization in scenarios where UAVs act as users of the mobile network. Adaptive height optimization has only been discussed in the scenario where UAVs act as BSs, supplementing the coverage of the mobile network. In this paper, we use Reinforcement Learning (RL) to dynamically optimize the UAV height once it moves in environments with different BS and building densities. RL has been shown to be well-suited to related problems where one does not have the complete information about the environment, such as horizontal trajectory planning for UAVs as users [8] and 3D positioning of UAVs as BSs [9].

The remainder of the paper is organized as follows. In Section II we discuss the existing work done on the issue of connectivity of UAVs to the wireless network. In Section III we present the system model, where we define how the UAV moves, how we model the antennas, building and BS distributions, and how we calculate the spectral efficiency. In Section IV we present the design and implementation of our proposed RL solution. Section V details the experimental setup. In Section VI, we evaluate our solution against a baseline, under BS and building density variations. We evaluate

how the different approaches affect the effective height of the UAVs and how they influence its spectral efficiency through the path. Finally, in Section VII, we conclude the paper and discuss the issues that remain open for future work.

II. RELATED WORK

In this section, we present work related to our approach to height optimisation of a UAV as a user of the network. We first present state of the art on the effect of interference on UAV connectivity followed by state of the art in UAV trajectory optimisation. We also introduce work on height optimisation in scenarios where UAVs are used as BSs.

In many examples of the prior art, works on UAV wireless connectivity, either for UAV as network end-user or UAV as BS, did not consider the effect of interference conditions. The quality of the link between UAV and a BS can suffer from interference coming from other BSs, from objects or buildings intercepting the directional connection between them (shadow zone), or even the natural fading on the propagation. The work in [10] considers UAV as BS and provides coverage to GUEs. In the paper, a UAV with an omnidirectional antenna flies over an urban area. The authors do not consider any source of interference, leaving the link limited with only the path loss. The authors propose a sigmoid model to investigate the probability of Line-of-Sight (LoS) channel in the UAV - GUE link as a function of the vertical angle between them. They concluded that a bigger angle decreases the probability of a building interfere on the link. They also add that there exists an optimal height for the UAV BS, which increases the coverage area. In the proposed work, we consider not only the building interference, but also the interference generated by other relevant BSs to the link UAV-GUE.

In [11], [12], authors applied stochastic geometry to model the coverage probability of a UAV BS network in a fading free and Nakagami-m fading channel. The authors fix the number of UAVs operating in an area at a certain height above the ground and demonstrate that with an increase in height, the coverage probability decreases. Also, in [12] authors demonstrate that bigger values of fading parameter reduce the variance of the Signal-to-Interference-and-Noise Ratio (SINR) for the GUE.

The initial research addressing UAV trajectory planning did not consider the optimisation of UAV height, but only the optimisation of its horizontal path. Works such as [13] propose a method for the UAVs to fly in an optimal route to its final destination, avoiding collisions. They apply Mixed-Integer Linear Programming (MILP) to aircraft collision avoidance. Their proposed solution can also be adapted to multiple waypoint path planning. An example of a proposal that has extra constraints is [14]. The authors consider the battery life of the UAV when planning the UAV path. The paper proposes a way for the UAV to fly without stopping to charge. The battery is charged on top of a building that charges them wirelessly. The UAV optimises its trajectory to be closer to these stations. These works open a challenge of trajectory optimisation for UAV as a user and bring different challenges interesting approaches to track the problem.

Although there are several works considering the UAV trajectory with different constraints, we found only two that considers the mobile network connections. In [15], the authors look at a cellular-connected UAV that needs to fly from an initial to a final location, while maintaining reliable communication with the underlying mobile network. It proposes horizontal trajectory optimisation approach to provide a reliable connection to the UAV while minimising the flight time between the two points. The approach assumes that the UAV would fly at the minimum height allowed by the regulatory entities. In this study, the authors also do not consider the interference from BSs to which the UAV is not connected and interference from the buildings blocking the link from UAV to BS. To accomplish the study objectives, a graph representation of the network is proposed, with 3 solutions: first, a graph where each node is a BS; second, a graph where the nodes are the handover points between the BSs; and third, where the handover points are the optimal point in an intersection area. Dijkstra algorithm is used to find the route of the UAV and show it is close to the optimal solution. The authors did not study how the height optimisation would affect their work. Still, they conclude that including a height variable to the problem is a not trivial task and that the graph solution is not the most appropriate one for 3D movement.

The work of [8] creates an optimised path with the objective to maintain always the connection to the BSs. This work discusses the importance of the altitude of the UAV and calculates the upper and lower bound that the UAV should fly at considering the known BSs locations. The exact height of the UAV is not calculated as it would increase the complexity of the algorithm exponentially, but only a range of heights the UAV should fly between to provide a minimum achievable rate. In addition, building blockage on the link UAV - BS is not considered. The solution is based on the game theory approach, where each UAV is a player. Deep RL algorithm based on echo state network (ESN) is used which guarantees the solution convergence. With this approach, each UAV decides its next location, where its action space corresponds to move to the left, right, forward, backwards or do not move. The authors conclude that the altitude is vital to minimise the transmission delay of the UAV and that it should be a function of the ground network density, network parameters, ground network data requirements and its action.

A UAV can have a different role on the cellular network, not being a user of the network but being part of it as a flying BS. In this role, the challenge is to provide a better quality of the link to GUE and the height optimisation is an important part of the solution. Although the height planning of UAV users is a new field, a few works study the height placement of UAVs as BSs. It is relevant to understand which techniques were successful in solving the height optimisation on that scenario as it can give a direction to solve the same issue for UAV as a user.

In [16], authors find an optimal position for a network of UAV as BSs in order to minimise the number of BSs required to provide the minimum quality of service for its users. The study consider the interference generated by buildings in an urban area to make their calculations and also NLOS

occurrences between the UAV and its users. However, on the paper the authors do not vary the parameters related to the density of the urban area on their investigations. They use particle swarm optimisation (PSO) algorithm as a solution to find the horizontal and vertical placement of the UAVs. The number of users on the network was essential to define the height and number of UAV as BS. The authors concluded that with their solution it is possible to decrease the amount of UAV as BS and provide the same quality on data rate. They also found that changing the height of the UAV they could increase and decrease the coverage area of the UAV as BS.

[9] proposes a 3 step solution for horizontal and vertical optimisation for UAV as BS with different machine learning (ML) algorithms for each step. The bounds the UAV height is the UAV maximum transmission power for its height, and the minimum required distance between the UAV and the users, defined by the regulatory entities, for the minimum height. In the beginning, it considers a static problem, where the users of the network do not move. First, it partitions the area into cells for the UAV-BSs to cover, by applying K-means (GAK-means) algorithm. Next, the authors use a Q-learning algorithm, where each UAV is an agent and has to decide its position by learning from its mistakes. Finally, they consider a scenario where users move between BSs and the network have to adapt to these movements. The authors apply Deep Q-Learning (DQN) as it enables each UAV to learn the dynamic movements of the users slowly. They conclude that the proposed solution outperforms the K-means algorithm and IGK algorithm with low complexity. The adaptation investigated at this work is similar to the problem of UAV as a user of the network, where the UAV has to adapt its path depending on the cellular network dynamism.

While some existing work has looked into optimising the height of UAV as BS, there is a significant lack of work looking at UAVs when they are the end users. In this work, we propose to optimise the altitude of the UAV based on the BS density (isolating the problem from a horizontal trajectory decision) to evaluate only the height of the UAV. We do it separated from the horizontal optimisation trajectory as previous works mentioned the complexity of adapting horizontal and vertical at the same time. We believe that filling this lack of the literature one could use our solution to optimise the height of the UAV and one of the horizontal trajectory optimisation strategies to complete the 3D path of the UAV from its initial to the final position. We also investigate how the density of buildings can influence the height of the UAV, being the first work, to our knowledge, that evaluates this relation between the optimal height of the UAV and building density distribution. To the best of our knowledge, this is the first work to dynamically and automatically adapt the best height of UAV as a user depending on the mobile network characteristics and building density.

III. SYSTEM MODEL

We consider an urban scenario where a UAV flies while connected to the cellular network. The UAV's initial position $(x_{i_{uav}}, h_{i_{uav}})$ and final position $(x_{f_{uav}}, h_{f_{uav}})$, where x

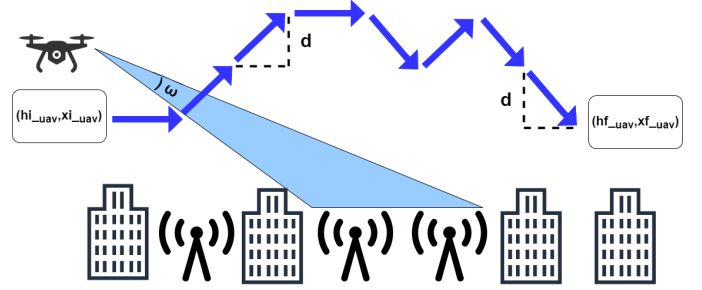


Fig. 1: Side view of a UAV connected to the mobile network when it moves up and down through the path in an urban area and in a horizontal straight line from position $(x_{i_{uav}}, h_{i_{uav}})$ to the final position $((x_{f_{uav}}, h_{f_{uav}}))$. The UAV has a directional antenna pointed to the BS that it is connected and will suffer interference from the BSs that are illuminated by the antenna beam pattern with beamwidth with angle ω .

refers to the coordinate of the UAV on the horizontal x axis, and h refers to its height, are known at the beginning of each topology, denoted as different distribution of BS and building. Its horizontal route is a straight line between the initial and final position, for ease of notation we assume that the start and end-points are both on the x -axis, with the y coordinate of the UAV remaining 0 at all times. The horizontal distance of the path is equal to $||x_{f_{uav}} - x_{i_{uav}}||$, the UAV travels this distance over a number of T timesteps, with a velocity of $v = ||x_{f_{uav}} - x_{i_{uav}}||/T$. The UAV height, h_{uav} , is going to be varied by our RL-based algorithm during the flight, as in Figure 1. The BS distribution follows a Poisson point process (PPP) with $\Phi = \{(x_1, y_1), (x_2, y_2), \dots\}$ of intensity BS_{dens} , at a height $h_b = \gamma_G$ above ground.

A. UAV and BS Antennas

The UAV is equipped with one omnidirectional antenna to detect BSs in the network and a directional antenna to connect to a serving BS and receive data. This scenario was adopted because the directional antenna can decrease the interference received by the UAV, as illustrated in our previous work [17] and in the 3rd Generation Partnership Program (3GPP) technical report [18]. Once we use the directional antenna we sacrifice environmental awareness in favour of a high-gain channel, so we use the omnidirectional antenna to detect pilot signals from BS in any direction.

The omnidirectional antenna has an omnidirectional radiation pattern, and it has an antenna gain equal to 1. The directional antenna has a horizontal and vertical beamwidth ω , represented in Figure 1, along with a rectangular radiation pattern; The antenna gain is defined as $\eta(\omega) = \eta(\omega) = 0$ outside of the main lobe; and $16\pi/(\omega^2)$ inside of the main lobe.

We express the coordinates of the BS which the UAV is associated with as $b_s = \{x_s, y_s\} \in \Phi$ and its horizontal distance to the UAV as r_s . Once the UAV chooses a BS to connect to, it aligns its directional antenna towards b_s ; the alignment forms an antenna radiation pattern around b_s . We define this antenna radiation pattern as $\mathcal{W} \subset r_s$. The directional antenna

forms an area, described in [17] and represented in Figure 1 as an blue shadow. The BSs that are inside the ring \mathcal{W} are denoted by the set $\Phi_{\mathcal{W}} = \{x \in \Phi : x \in \mathcal{W}\}$. The signals from the BSs that are inside the ring generates interference to the link UAV to selected BS.

The UAVs are modelled as having a steerable directional antenna with fixed radiation pattern which is down-tilted towards the associated BS with angle ϕ , which is also the vertical angle between the UAV and the BS, with its design and propagation described in [19]. We assume a Uniform Linear Array (ULA) of N_t antenna elements that have omnidirectional antenna gain on the horizontal plane and have a vertical antenna gain as given in [19].

B. Building distribution

The buildings distributed in the area might affect the UAV LoS, as they can block the channel between the UAV and the BSs. If the signal is blocked by a building, non-Line-of-Sight (NLoS), which causes the signal to be attenuated, which is reflected in the SINR expression in Equation 1. We use a commonly-adopted model for the urban environment which models the buildings as a square grid with the locations of building centerpoints (x_{bl}, y_{bl}) , that was presented in [20] and used in works as [16], [21], [22]. The area occupied by each building, Bl_a , is constant, and the density of buildings, $Build_{dens}$, is denominated by the number of building per square kilometre. The individual building height, h_{bl} is randomly distributed according to a Rayleigh distribution, with scale parameter a .

C. UAV-BS Link

Spectrum efficiency is the maximum bit rate that can be transmitted per unit of bandwidth and is a measure of the quality of service that can be served by that part of the network. The ShannonHartley theorem bounds the maximum achievable rate a user can reach once it establishes a wireless link. As we want to improve user's experience providing reliable connectivity to UAVs, our purpose is to increase spectrum efficiency. We calculate the spectrum efficiency value for the calculated SINR based on ShannonHartley theorem. The SINR is a function of the antenna gain and channel model and given as:

$$SINR = \frac{p\eta(\omega)\mu(\phi)c(x_s^2 + \Delta\gamma^2)^{-\alpha_{t_s}/2}}{I_L + I_N + \sigma^2} \quad (1)$$

where p is the BS transmit power, μ is the antenna gain, α_{t_s} is the pathloss exponent, $t_s \in \{L, N\}$ indicates whether the UAV has LoS or NLoS to its serving BS x_s , c is the near-field pathloss, σ^2 is the noise power, and I_L and I_N are the aggregate interference from LoS and NLoS, respectively.

The UAV connects to the BS at the shortest horizontal distance at all times (as this allows it to limit the received interference [17]). Therefore, as the UAV moves through the environment some BSs become closer and others more distant. When it reaches the point where its serving BS is no longer the closest BS, it will reconnect to the new closest BS. We assume that this handover occurs seamlessly, and there is no disconnect or loss of signal quality when it happens.

IV. REINFORCEMENT LEARNING APPROACH

In this section, we detail the proposed algorithm we use in our solution. To solve the height optimisation problem for a specific position of the UAV in a particular topology of the BSs and buildings, one could apply stochastic geometry to calculate the optimal height of the UAV as in [17]. The main issue to this approach is that to represent this problem in statistic geometry, one has to know the statistical distribution of the features of the environment for each position that the UAV assumes through its path. This can be computationally expensive to run and the environment might not be a perfect expression of what the UAV would find once its flying in real world, as any error on the environment description would lead to a wrong calculation.

To tackle this issue our solution is based on DQN, a commonly used model-free RL approach. DQN does not need a predefined model of the environment and it learns once it interacts with it. DQN can manage to provide a solution without all the environmental constraints. RL has been previously successfully applied in problems similar to ours. For example, in [8], authors apply RL to horizontal trajectory optimisation, and in [9] RL showed to be efficient on the height optimisation for the scenario where a UAV BS was positioned to serve ground.

Q-learning is an RL algorithm that enables an agent to learn how to choose an action to take with respect to a long-term reward [23]. We apply DQN algorithm that learns a policy, π , and tells the agent which action to take. DQN originated from the Q-learning algorithm due to the complexity of the former when dealing with a big number of possible states. In classical Q-learning a Q-table would be learned, which maps the Q-values of each action for a given state. The issue is that for several real-world problems (such as this one) the number of states is prohibitively large for classical Q-tables, and so the neural network is used to approximate the Q-table mapping.

DQN uses a Neural Network (NN) to solve non linear problems. This technique utilises rewards to train the algorithm to take the appropriate action for a given state. A reward is a scalar value received after each action for transition to the new state, which the agent uses to learn best action to take in each state. The algorithm calculates the quality of each action on a specific state, the Q-value, in order to learn which is the best action on that state. A Q-value is the expected value of an action considering a long term reward if taking that action at that state.

We also apply experience replay, presented in [24], which aims to make more efficient use of previous experience as the agent can reuse and remember them. This technique is applicable when it is necessary to make the learning converge faster, thus minimising the interactions with the environment.

The main components required for an RL representation of the problem are an agent, state space, action space, and environment reward. We define those below:

- Agent: the entity that takes actions and which is under our control; it is the UAV, in this case.
- State Space - S: is the set of observations from the environment that the agent receives before and after

taking action. We have to choose the environmental information that is relevant to the problem and define in S . To evaluate the impact of including individual parts of a state and identify minimum sufficient state information, we perform experiments using various combinations of environment information captured in S , including BS_{dens} , $Build_{dens}$, $SINR_{cand}$, r_s , h_{uav} . We list these specific scenarios in Section IV-A.

- Action Space - A: the set of all possible actions that the UAV can take. An action a will be taken at the end of each time-step. They are defined as:

$$a = \{0, 1, 2\} \quad (2)$$

where:

- 0 = move up
- 1 = move down
- 2 = do not change height

- Reward - R: as the primary goal of our approach is to improve the UAV spectral efficiency during flight; our reward function has to express it. We define the reward function as a function of spectrum efficiency defined by the ShannonHartley theorem.
- ϵ : during the training, DQN algorithm needs to explore the possible actions it can take in order to find the optimal policy. ϵ is the greed policy used to determine when the algorithm should use the neural network to choose an action, and when it should explore by selecting an action at random. In our solution, we design a $\epsilon = 1$, where we select an action at random, and we decrease it until 0.001 during the training process.

A. DQN State Space variations

As described above, an agent's state needs to encode all of the information relevant for an agent to make a decision. In this section we discuss the relevance of different environment information for our approach, and based on this define four different state spaces, mapping to four different evaluation scenarios, in order to assess their impact on the learnt solution.

The SINR of the wireless link to the serving BS is relevant to the UAV, and it is available to the UAV as a user of the network. As typical ground users measure the SINR of signals from nearby BSs, we assume this information is always available to the UAV to use for the algorithm.

The UAV also should have any related information to its path, including its current height (h_{uav}). Considering that we want to define the height on the next time-step, we use height as a parameter of our state information.

There is network data that could be useful to a UAV that is flying over an area. The location of BSs in a city, defined as (BS_{loc}), is important and relevant data to the UAV it could be sent by the network operators for more precise and up to date data. We use the distances of the closest BSs, (r_s), to the UAV as a set of inputs.

The density of the BS (BS_{dens}) can be calculated with the number of BSs in an area. It can influence the interference at

the UAV, so it is studied to check how relevant it is in the height optimisation in our RL solution.

As mentioned in Section III, the building density ($Build_{dens}$) can influence the UAV link to the BS. The $Build_{dens}$ is data that could be acquired from the city map, so we also check its influence in the height optimisation decision.

We propose 4 different approaches to understand how each piece of environmental information is relevant to our investigation. Each of the 4 solutions considers different characteristics of the environment to make its decisions. Below there is a summary of the 4 approaches used in our investigation:

- State_Basic = [$SINR_{cand}$, h_{uav} , r_s]
- State_BS = [$SINR_{cand}$, h_{uav} , r_s , BS_{dens}]
- State_Build = [$SINR_{cand}$, h_{uav} , r_s , $Build_{dens}$]
- State_Complete = [$SINR_{cand}$, h_{uav} , r_s , BS_{dens} , $Build_{dens}$]

B. DQN algorithm

The pseudo-code of the DQN algorithm to optimise h_{uav} is shown in 1.

First, it is necessary to initialise the models, setting up their configurations and hyper-parameters. Then, for different BS and building densities, we create the city topology. Before taking an action, it is necessary to collect information of the environment, described in line 5. To take an action, we apply the greedy approach for RL. The greedy approach is a method to balance exploration and exploitation in an RL model. Usually, as in our example, a random number is chosen and compared to a constant (epsilon), where epsilon is the probability of choosing to explore the environment. Exploration helps the agent to improve its knowledge of the environment and avoid converging on sub-optimal behaviour. The epsilon-greedy approach balances exploitation and exploration behaviour. Once the action is chosen, we move the UAV horizontally (x_{uav}) and vertically (h_{uav}) for the next time step. At the end of each timestep the model is retrained.

In our algorithm, we apply use experience replay for more efficient use of experience samples. This replay stores in the buffer, β , the state, action, reward and next state at each timestep. As the DQN is run over a number of episodes this experience replay becomes populated with entries. At the end of each timestep, we sample random entries from this experience replay, and feed them to our DQN for training if the buffer has at least a minimum defined size (β_{min}). Once the episode is finished, it goes for another episode round.

V. EXPERIMENT DESIGN

To evaluate our proposed approach and analyse how the city topology influences the connected UAV, we utilise the simulator developed in R used in [17].

During the experiments, we do not vary the BS and the building densities at the same time, always letting one of the variables to remain fixed. The chosen value to be the fixed is the mean of the list values, and it is expressed in Table I with other simulation parameters. A step (or timestep) is a single movement (action taken) of the UAV in a specific BS and building topology. An episode consists of 100 steps. In the

Algorithm 1 DQN algorithm and simulation

Input: $S = [SINR_{cand}, h_{uav}, r_s]$; $BS_{dens}, Build_{dens}$; β ; β_{min}

Output: UAV_{h+1}

```

1: Initialise.Model
2: Generate.City.Topology( $BS_{dens}, Build_{dens}$ )
3: for  $i$  in  $1:episodes$  do
4:   for  $j$  in  $1:steps$  do
5:      $s \leftarrow State.Information$ 
6:     if  $Random.Number(0-1) > epsilon$  then
7:        $action \leftarrow Model.Predict.Best.Action(s)$ 
8:     else
9:        $action \leftarrow Random[Up, Down, Do.Not.Move]$ 
10:    end if
11:    if  $action = up$  then
12:       $h_{uav} \leftarrow h_{uav} + d$ 
13:    else if  $action = down$  then
14:       $h_{uav} \leftarrow h_{uav} - d$ 
15:    else
16:       $h_{uav} \leftarrow h_{uav}$ 
17:    end if
18:     $x_{uav} \leftarrow x_{uav} + 1$ 
19:     $R \leftarrow \log_2(1 + S/(N + I))$ 
20:     $epsilon \leftarrow epsilon * epsilonDecay$ 
21:    Store.Transition( $\beta$ )
22:    if  $length(\beta) > \beta_{min}$  then
23:      Sample.Batch( $\beta$ )
24:      Train.Model( $Q_{value}$ )
25:      Update( $R$ )
26:    end if
27:  end for
28: end for

```

beginning of an episode h_{uav} is fixed for all approaches, and afterwards it is controlled by the RL algorithm action selection process or the baseline solution algorithm.

We choose 3 different height-selection strategies to benchmark the performance of our approach. For the first one, we use one of the most common approaches to UAV height selection [2], [4], [5], [13] which is to maintain a constant height throughout the entire trajectory. We pick 100 meters to be our fixed height, as it is the halfway value between the ground and our maximum height that is 200 m, as described in I.

The second baseline is for the UAV to randomly take an action every step. We want to investigate how well a random decision can perform and check if our solution is actually learning and not acting randomly.

The last baseline is a genie-assisted solution. In the genie-assisted approach, the UAV knows whether the maximum SINR in the next time step will be found above or below its current height, and will move up or down depending on this location. We assume the genie-assisted solution as the best solution in the baseline as it has a priori information of the environment.

Variable	Value
h_{uav}	100m
BS_{dens}	$[1, 5, 10]/km^2$
Bs height $h_b = \gamma_G$	30m
$Build_{dens}$	$[1, 5, 10] * 100/km^2$
Building area Bl_a	$40m^2$
BS downtilt ϕ	10
Simulated area	$25km^2$
velocity	10 m/s
timestep	1 s
UAV travel distance	1000 m
step	100
Allowed UAV height range	$[20 - 200]m$
Building height parameter a	20m
d	7 m

TABLE I: Variables used in the environment simulation and their values.

Variable	Value
steps per episode	100
episodes	300
epsilon	1
epsilon_decay	0.99

TABLE II: Variables used on the RL model and their values.

VI. EVALUATION

The main points that we want to evaluate are how the BS density and building densities influence the optimal height of a connected UAV. In order to assess each of these factors separately, we divide this section in the two subsections. First, we analyse the achievable throughput by BS density and building density, then we inspect height changes within each approach more closely.

A. Achievable throughput

In this subsection we analyse the achievable throughput per unit of bandwidth, that is a sum of the spectrum efficiency over an entire episode, for varying BS densities and building densities.

1) *BS density*: To demonstrate how the RL solution can increase performance through the different BS densities we study in detail three different BS densities $(1, 5, 10)/km^2$, denoted as low, medium and high. Figure 2 show the three scenarios where we evaluate the achievable throughput (bits/Hz) of each solution per number of episodes.

As an overall analysis of the RL approaches in Figure 2, they need a number of episodes to learn the best behaviour for the specific BS density due to the nature of RL, in that it takes a number of episodes for the algorithm to learn. In 2a for low BS density, the RL solution overpasses the genie approach in around 75 episodes, and for high BS density, in Figure 2c, it also overpasses around the same epochs. This analysis is not clear once we analyse Figure 2b, where not all the solutions overpass the Genie Assisted approach and the learning curve is not so sharp. When compared to the Constant and random approaches the model starts with better performance for medium and high BS densities, and for low it overpass quickly, after less than 50 episodes to provide a consistent improvement of the achievable throughput.

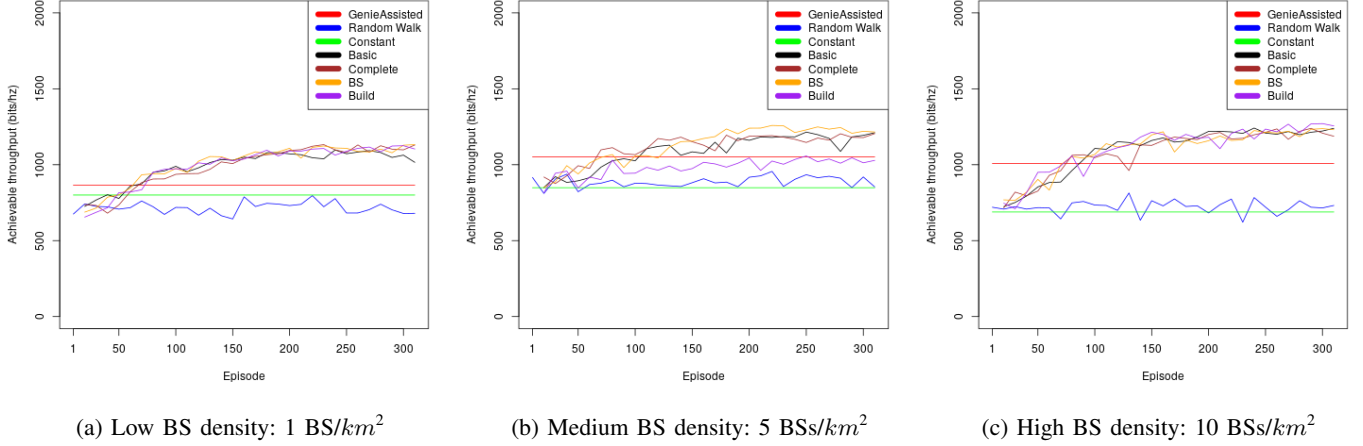


Fig. 2: Achievable throughput per unit of bandwidth (bits/Hz) per episodes for different BS density and constant building density of $500/km^2$.

To analyse how the solutions perform after training and in a macro point of view, Figure 3 shows the average achievable throughput and standard deviation per BS density. Figure 3 show that the Random approach is comparable to the performance of the Constant baseline for all the BS densities, being never far from the Constant achievable throughput. The Constant solution shows that for low BS densities it is comparable to the Genie Assisted approach with a difference of 65 bits/Hz, although for the medium and higher BS densities, it has a considerably worse performance, being 205 bits/Hz for medium and about 320 bits/Hz for high BS densities. This result shows that for higher BS densities it is necessary to have a more complex solution to provide a better rate to the UAV. The Genie Assisted approach always has a better performance compared to the Constant and Random approaches, because this solution can predict which vertical direction the highest SINR is to be found in, in the next time-step.

For low BS density distributions, all of the RL algorithms provide better achievable throughput than the baseline solutions, achieving 290 bits/Hz on average more when compared to the Constant approach. For medium BS distribution, the RL algorithms still provide a better solution than the Constant and Random approaches, but not all of them surpass the Genie Assisted approach, that has additional information about the environment. The Basic and BS solution provide 125 bits/Hz of improvement in achievable throughput when compared to the Genie Assisted approach, and the BS provide 185 bits/Hz of improvement. The Building approach provides an achievable throughput compared to the Genie Assisted approach. This changes once the scenario comes to a high BS density, when the RL solutions provide an increase of about 200 bits/Hz when compared to the Genie Assisted approach, and 520 bits/Hz when compared to the constant approach. The Figure 3 does not show any strong differences between the RL solutions, for most cases, showing that the RL approach can deal well with a lack of detailed information from the environment.

Figure 3 illustrates that the RL solutions always maintain

an average achievable throughput between 1095 and 1210 bits/Hz, which provides an the expected achievable throughput to the user and shows that once the BS density increases, there is a small improvement on the achievable throughput, being 60 bits/Hz for medium and 55 bits/Hz when changes from medium to high BS density.

The differences between the RL approaches are smaller compared to the baselines, although, they are visible in Figure 3. For lower densities the RL solution with the Basic space input, with just the information that is already available to cellular network users, achieves 205 bits/Hz of improvement when compared to the Genie Assisted approach. Although, when compared to the other RL solutions, it achieves 30 bits/Hz less, indicating that for lower densities the 3 solutions with some type of extra information perform better. Between themselves, the achievable throughput does not vary more than 7 bits/Hz. For medium BS density the quality of approaches diverges, showing that the BS solution is the best, exceeding the Build solution by 215 bits/Hz. This result shows that the information of building density does not help the UAV to make decisions once we vary BS density. However, it influence is visible for medium BS density, for low and high the Build solution is comparable to the other RL approaches. The small differences between the solutions happen as an adjustment of the environment, but mostly all the solutions are inside the standard deviation, as showed in the figure.

B. Building density

In this subsection we evaluate how the building density impacts the overall achievable throughput. To the best of the authors knowledge, this is the first work to evaluate how the building density affects the UAV achievable throughput per unit of bandwidth.

Similar to section VI-A1, in this section we investigate how the RL solution can increase achievable throughput performance for the different building densities. We evaluate the two different building densities $(1,10)*100/km^2$, to evaluate

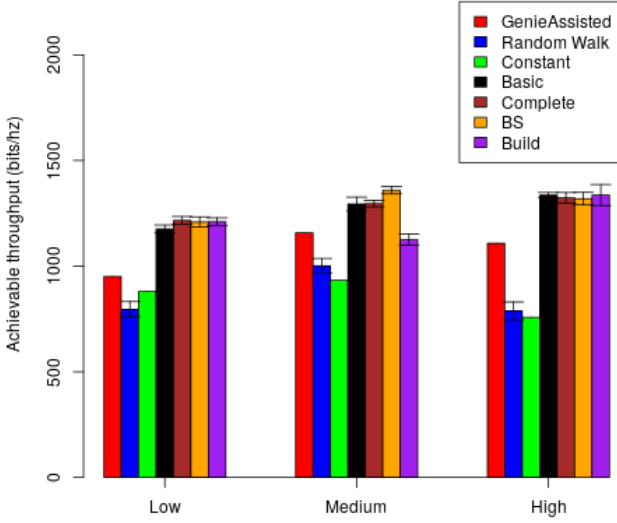


Fig. 3: Achievable throughput per unit of bandwidth (bits/Hz) per BS density ([1,5,10]BS/km²)

the low and high building density distributions. The medium one is analogous to the analyses in VI-A1. Figure 4 illustrates two scenarios where we assess the achievable throughput of each solution per number of episodes.

Figure 4 shows the learning curve of the RL models once we vary building density. For low building density, in Figure 4a, it is easier to see the learning curve and when most of the solutions overpass the Genie Assisted approach, which is around the 100 episodes point, 25 more than compared to low BS density. The number of BSs influences directly the number of interfering BS in the scenario. Once we vary building density, we influence the number of BSs that will be blocked by the buildings, generating less interference from undesirable BSs. As this relationship is less obvious than the number of BSs, the model takes longer to adapt to these variations. For high building density, in Figure 4b, the learning curve is more attenuated, but it also already starts with a better performance when compared to the Constant and Random solutions.

Figure 5 is a macro view of the performance of the solutions over the building densities, showing only the RL values after the model is trained. The Random approach once we vary the building density has its achievable throughput always comparable in performance to the Constant approach, as Figure 5 shows. The Constant solution has a low average achievable throughput for low densities of buildings, achieving 420 bits/Hz. It improves once the building density increases going to 850 and 870 bits/Hz, for medium and high building densities, respectively. The Genie Assisted approach always has a better performance compared to the Constant and Random approaches, as expected. For low building density when compared to the Constant approach it can achieve 400 bits/Hz

of increase in throughput, and for high building densities surpass the Constant approach in 250 bits/Hz.

In Figure 5, all of the RL algorithms provide better achievable throughput than the baseline solutions, achieving 530 bits/Hz on average more when compared to the Constant approach, doubling the achievable throughput for lower densities of building. Once we look to the medium building distribution, most of the RL algorithms still provide a better solution than the Genie Assisted approach. The build solution is the only one that provides comparable achievable throughput to the Genie Assisted solution, showing a worse performance than the other RL algorithms. When the scenario has high building density, the RL approaches again provide similar achievable throughput, the Basic, BS and Complete solutions being inside their standard deviations. The exception is again the Build solution, which provides worse performance once compared to the other RL approaches. We believe that including the building density in the model once we increase the building density makes it harder to learn that with more buildings, the UAV will have less interference as the signals coming from undesirable BSs would be blocked. Further investigation to analyse how to use this information as input is needed.

1) *Height adaptation:* In this section, we investigate how the different approaches behave throughout a single episode and through the different BS and building densities, showing how these solutions change the UAV heights.

First we analyse the learning process through 2 different episodes. As each topology was run for 300 episodes, we do not show heights for all episodes, but analyse only the behaviour in episode 1, when the RL agent is exploring the environment, and the final episode 300, when the learnt behaviour has converged, as illustrated in Figure 6.

Figure 6a shows that the RL solutions do not follow any specific behaviour, it happens because in this early episode, we apply the greedy approach with a large value of ϵ , which means that most actions taken by the RL algorithm are random. Figure 6b shows how these random actions influence the spectral efficiency through the path. The main point is that the RL solution should adapt to these changes after learning more about that topology.

Figure 6c shows that the RL solutions adapted well to the scenario, and all of them follow the same time-varying height trajectory of the UAV. It is expressed in their spectral efficiencies in Figure 6d, where the average of mean spectral efficiency for the RL approaches increased 27%. This confirms that the RL approaches are learning appropriate decision-making to adjust the height while travelling through that environment, and not acting randomly as in the first episode of this distribution.

Figure 7 shows how the BS and building densities affect the average chosen UAV heights for all the approaches. The genie approach solution, maintains lower height than the other solutions for all the cases. For most cases of all the other solutions, they maintain around 100 m height, which shows that the assumed Constant solution is adequate to our analysis. Although they usually maintain an average height of 100 m, once we analysed the throughput of the Constant solution we note that most of the time it is the worst approach, being

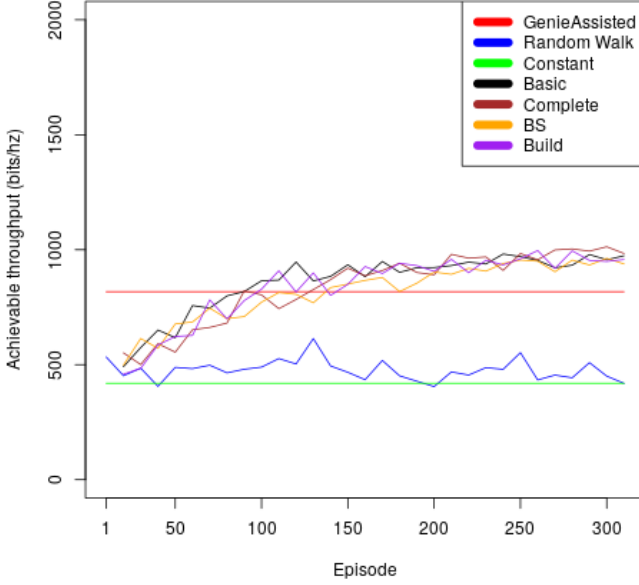
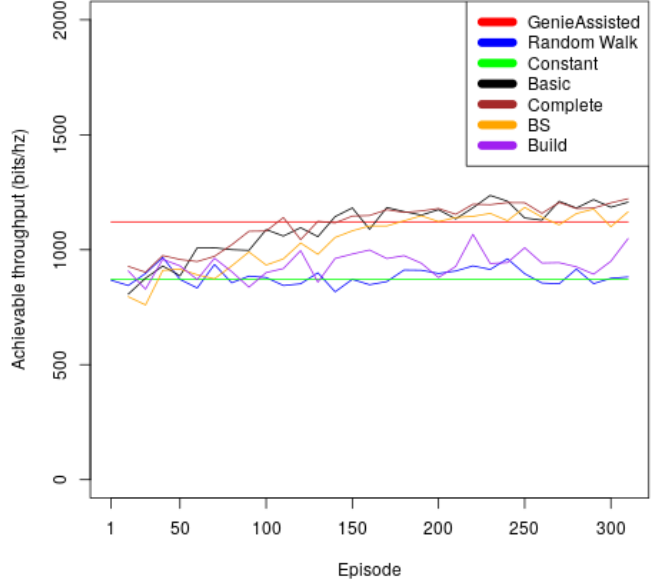
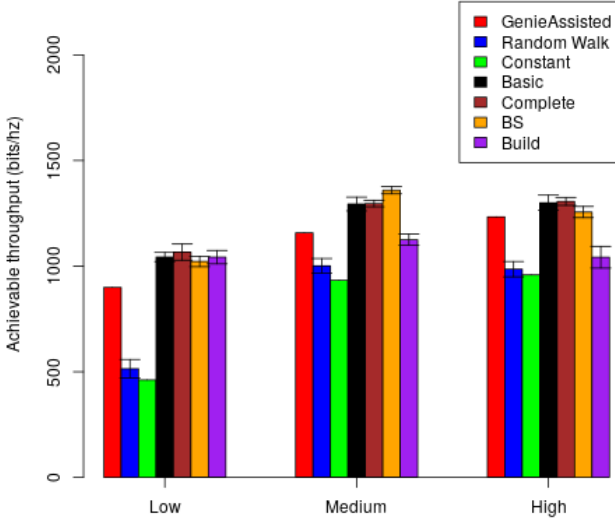
(a) Low building density: $100/km^2$ (b) High building density: $1000/km^2$

Fig. 4: Achievable throughput per unit of bandwidth (bits/Hz) per episode for different building density.

Fig. 5: Achievable throughput per unit of bandwidth (bits/Hz) per building density ($100/km^2$, for low, $500/km^2$ for medium, and $1000/km^2$ for high), and BS density fixed in $5/km^2$.

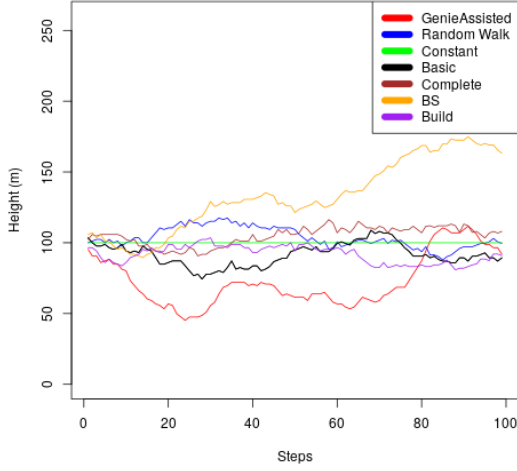
better only when compared to the random approach. It shows that some height adaptation to the environment is necessary to provide a better throughput to the connected UAV. The RL solutions usually maintain the UAV at slightly higher altitudes, which shows in a better achievable throughput performance

compared to the baselines. For higher building densities, the RL solutions resulted in considerably higher altitudes, being around 140 m, which shows that even at greater heights it is possible for the UAV to achieve good throughput.

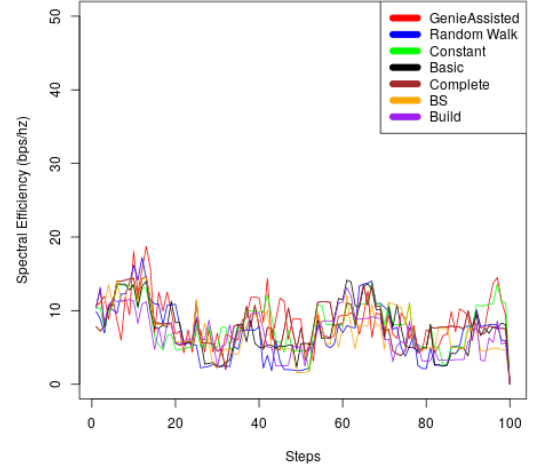
Observing behaviours for both BS and building densities, we conclude that RL is an adequate approach to solve UAV height optimisation. On Figures 6a and 6c, the RL solutions were demonstrated to be learning a path, resulting in a spectral efficiency improvement. For most of the cases, the RL solutions have a better performance than the baseline approaches. For low BS density, the RL approaches achieve up to 25% improvement compared to the Genie Assisted approach, and for low building density up to 125% of improvement when compared to the Constant approach.

VII. CONCLUSION

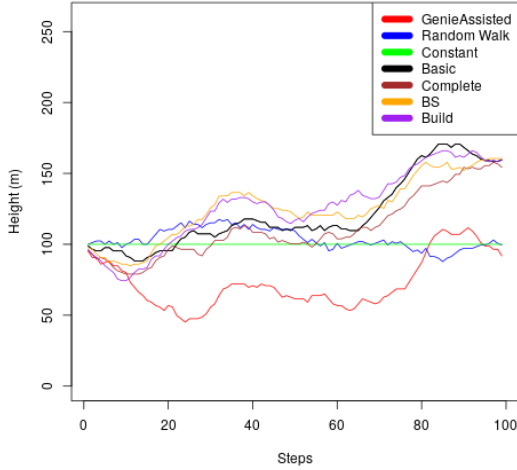
In this paper, we have presented an RL approach to solve UAV height optimisation given different BS and building densities for a moving UAV which is acting as a user of the cellular network. Our main focus was to increase the throughput of the UAV for different city topologies by allowing the UAV to vary its height inside a range. We investigated how different state information provided as an input to the RL algorithm can influence the spectral efficiency once we vary the BS and building densities. The simulated environment is complex, with the received channel quality affected by distance attenuation of the signal, building blockage, interference, and the antenna gain of both the BS and the UAV antennas. Changing the height will change all of these factors, some will improve, and some will deteriorate. Because of this complexity, it is not evident if a higher altitude will always provide better



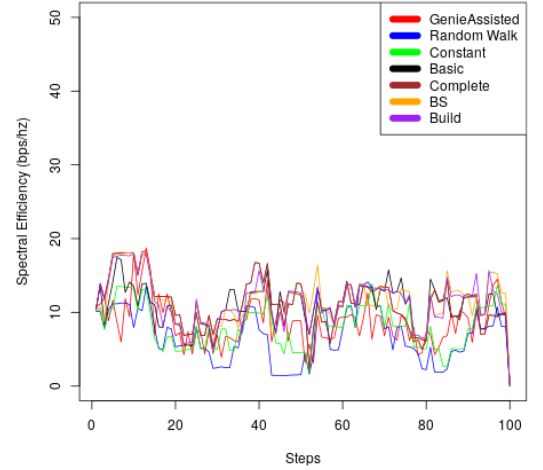
(a) Height of the UAV in meters through 100 steps in the first episode



(b) Spectrum efficiency in bps/Hz through 100 steps in the first episode



(c) Height of the UAV in meters through 100 steps in the episode 300



(d) Spectrum efficiency in bps/Hz through 100 steps in the episode 300

Fig. 6: Height of the UAV and Spectrum efficiency per step for 1 BSs/ km^2 and 500 buildings/ km^2 .

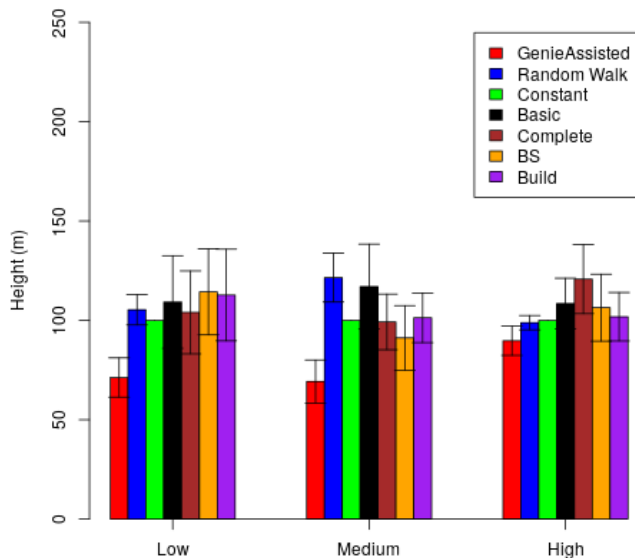
throughput; the height needs to be adjusted for each individual environment.

In our analysis, we concluded that for low densities of BS and buildings, all of the RL models had similar performance, but once we increased the building density, the solution with building density information as input had a worse performance, showing that this information was not helpful to improve the RL algorithm performance. However, the building density was shown to influence the achievable throughput and height of UAV, being an important factor to analyse once one investigates the connected UAV path optimisation.

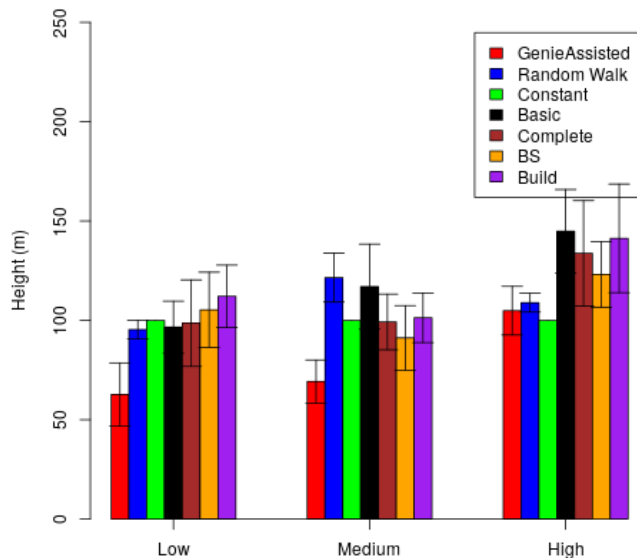
Observing behaviours for both BS and building densities, we found that RL is a satisfactory approach to accomplish UAV height optimisation. On the single-episode per step analysis, we could observe the learning of the algorithm,

starting from random movements, to when it learns a path that increases its spectral efficiency by 27%. For a greater number of the investigated topologies, on average, the RL exceeds the baseline approaches, achieving 530 bits/Hz higher throughput compared to the Constant approach and 130 bits/Hz compared to the Genie Assisted approach, for BS densities equal to 5/ km^2 and 100 buildings/ km^2 .

Although we did an extensive analysis of the building and BS densities, and we follow a commonly used simulation model for the urban environment, we believe that implementing this evaluation on city maps of existing cities might provide some variance in the results. As future work, our RL approach will be evaluated in scenarios based on real data of BS locations and city maps. An additional challenge that we intend to investigate in the future is how to jointly adapt the



(a) Height per BS density



(b) Height per building density

Fig. 7: Height per BS and building densities.

horizontal and vertical trajectory of a UAV as a user of the cellular network in order to increase spectral efficiency. We will also investigate the performance of an algorithm trained on one density once it encounters a different density (both BS and buildings), to simulate, for example, a transition from an urban to suburban area during the flight. Another aspect that can be investigated is the choice of which BS the UAV connects to so that the network is not negatively impacted by handover effects. The selection of the connected BS can also be optimised in order to increase spectral efficiency in the long term, considering the penalties introduced by frequent BS handovers.

ACKNOWLEDGEMENTS

The research leading to this work received funding from the European Horizon 2020 Program under the grant agreement No. 732174 (ORCA project). In addition, this work was partly funded by Science Foundation Ireland (SFI) and the National Natural Science Foundation of China (NSFC) under the SFI-NSFC Partnership Programme Grant Number 17/NSFC/5224.

REFERENCES

- [1] "3rd Generation Partnership Project Technical Specification Group Radio Access Network," 3GPP, Tech. Rep., March 2017.
- [2] Mozaffari, Mohammad *et al.*, "A tutorial on UAVs for wireless networks: Applications, challenges, and open problems," *IEEE Communications Surveys & Tutorials*, 2019.
- [3] —, "Unmanned aerial vehicle with underlaid device-to-device communications: Performance and tradeoffs," *IEEE Transactions on Wireless Communications*, 2016.
- [4] M. M. Azari *et al.*, "Reshaping cellular networks for the sky: Major factors and feasibility," in *2018 IEEE International Conference on Communications (ICC)*. IEEE, 2018, pp. 1–7.
- [5] —, "Coexistence of terrestrial and aerial users in cellular networks," in *2017 IEEE Globecom Workshops (GC Wkshps)*. IEEE, 2017, pp. 1–6.
- [6] "Unmanned aircraft systems," Qualcomm, Tech. Rep., May 2017.
- [7] R. Amer *et al.*, "Mobility in the sky: Performance and mobility analysis for cellular-connected uavs," *IEEE Transactions on Communications*, vol. 68, no. 5, pp. 3229–3246, 2020.
- [8] U. Challita *et al.*, "Cellular-connected uavs over 5g: Deep reinforcement learning for interference management," *arXiv preprint arXiv:1801.05500*, 2018.
- [9] X. Liu *et al.*, "Reinforcement learning in multiple-uav networks: Deployment and movement design," *IEEE Transactions on Vehicular Technology*, vol. 68, no. 8, pp. 8036–8049, 2019.
- [10] A. Al-Hourani *et al.*, "Optimal lap altitude for maximum coverage," *IEEE Wireless Communications Letters*, vol. 3, no. 6, pp. 569–572, 2014.
- [11] V. V. C. Ravi and H. S. Dhillon, "Downlink coverage probability in a finite network of unmanned aerial vehicle (uav) base stations," in *2016 IEEE 17th International Workshop on Signal Processing Advances in Wireless Communications (SPAWC)*. IEEE, 2016, pp. 1–5.
- [12] V. V. Chetlur and H. S. Dhillon, "Downlink coverage analysis for a finite 3-d wireless network of unmanned aerial vehicles," *IEEE Transactions on Communications*, vol. 65, no. 10, pp. 4543–4558, 2017.
- [13] A. Richards and J. P. How, "Aircraft trajectory planning with collision avoidance using mixed integer linear programming," in *Proceedings of the 2002 American Control Conference (IEEE Cat. No.CH37301)*, vol. 3, 2002, pp. 1936–1941 vol.3.
- [14] E. Natalizio *et al.*, "Download and fly: An online solution for the uav 3d trajectory planning problem in smart cities," in *Proceedings of the 9th ACM Symposium on Design and Analysis of Intelligent Vehicular Networks and Applications*, 2019, pp. 49–56.
- [15] S. Zhang *et al.*, "Cellular-enabled uav communication: A connectivity-constrained trajectory optimization perspective," *IEEE Transactions on Communications*, vol. 67, no. 3, pp. 2580–2604, 2019.
- [16] E. Kalantari *et al.*, "On the number and 3d placement of drone base stations in wireless cellular networks," in *2016 IEEE 84th Vehicular Technology Conference (VTC-Fall)*, 2016, pp. 1–6.
- [17] B. Galkin *et al.*, "Backhaul for low-altitude uavs in urban environments," in *2018 IEEE International Conference on Communications (ICC)*. IEEE, 2018, pp. 1–6.
- [18] "Tr 36.777: Technical specification group radio access network; study on enhanced lte support for aerial vehicles (release 15)," 3GPP, Tech. Rep., 2018.

- [19] R. Amer *et al.*, "Performance analysis of mobile cellular-connected drones under practical antenna configurations," in *2020 IEEE International Conference on Communications (ICC)*. IEEE, 2020.
- [20] "Recommendation P.1410-5 "Propagation Data and Prediction Methods Required for the Design of Terrestrial Broadband Radio Access Systems Operating in a Frequency Range From 3 to 60 GHz"," ITU-R, Tech. Rep., 2012.
- [21] B. Galkin *et al.*, "Coverage analysis for low-altitude uav networks in urban environments," in *GLOBECOM 2017-2017 IEEE Global Communications Conference*. IEEE, 2017, pp. 1–6.
- [22] R. I. Bor-Yaliniz *et al.*, "Efficient 3-d placement of an aerial base station in next generation cellular networks," in *2016 IEEE International Conference on Communications (ICC)*, 2016, pp. 1–5.
- [23] C. J. C. H. Watkins, "Learning from delayed rewards," 1989.
- [24] T. Schaul *et al.*, "Prioritized experience replay," *arXiv preprint arXiv:1511.05952*, 2015.